OBSERVATIONS OF SOLAR RADIO EMISSION AT 9.4 Gc/s BY 16-ELEMENT INTERFEROMETER

by
HARUO TANAKA

Summary–16-element interferometer for use at 9.4 Gc/s was completed in the early summer of 1960. Maximum resolving power is 2.2′. Observations for more than 5 hours are being conducted every day. The most remarkable feature is the capability of taking 2 series of drift curves for both brightness and circular polarization. Bipolar nature of the source of polarization over the bipolar sunspot has now become clear. Size of a radio spot at this frequency seems to be not much larger than the area of optical sunspot in contrast with more diffused feature observed at lower frequencies. The size does not change appreciably during its travel across the solar disk. Some centers of polarization were found to shift during the 2nd phase of the cm wave burst, probably due to the change of emission mechanism.

1. Introduction

Regular observations of the sun using an 8-element interferometer for use at 9.4 Gc/s[1] have been conducted for about a year in parallel with the observations by another similar equipment for use at 4 Gc/s[2] and some interesting results have been obtained[3]. The former was extended to 16 elements in the early summer of 1960. Maximum resolving power was increased from 4.5 to 2.2 minutes of arc. This may be the first interferometer that can observe the distribution of the sources of polarization as well as the brightness over the solar disk at the same time. Though the resolving power is still poor for the observation of detailed features of radio sources, it will be covered to a certain extent with the simple beam configuration as well as the precise observations for a long time, more than 5 hours every day.

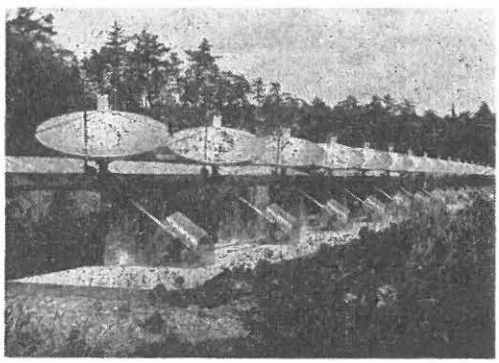

Fig. 1. General view of 16-element interferometer.

II. Equipment

1. Antenna

16 paraboloids, 2 meters in diameter, are placed in E–W direction at 2.74 meters' interval as shown in Fig. 1. Each polar axis is fixed on a concrete basis of 43 meters in total length, and is driven by a common shaft of 0.03 rpm. This common shaft is divided into unit pieces which are free in axial direction, whereas play of rotation is negligible. The concrete basis is now well aged and each mount has the accuracy of 1 millimeter in every direction. though correction by a few millimeters was necessary several months after construction.

Antenna feeds are H_{11} matched circular waveguide ends for receiving circularly polarized components. The half-power width of the main beam is 2.22′ for beam number 0 around local noon, 2.44′ for number 30, 3.01′ for number 50 which is placed approximately 2.5 hours before and after local noon. These values are calculated for noise signals of 8.5 Mc/s band width[2].

2. Device for measuring polarization

16 ferrite switches with quarter-wavelength plates[4] are placed in cylindrical boxes over the paraboloids. Square-wave current is fed in series into the coils so that the right and left handed polarized components (hereafter will be called R and L) are switched at a speed of 125 c/s. Through a phase sensitive detector at the output of the receiver, we can get a drift curve of R–L.

3. Transmission lines

As shown in Fig. 2, the outputs of the antenna are divided into two parts and each of the 8 outputs is combined in a conventional form with silver coated rigid waveguides. Contact couplings are used for simplicity, which are air-tightened by applying silicone grease over the contact surfaces. Each output passes through 2 rotary joints and 3 magic tees. The total loss measured by comparing effective temperature with that of the horn antenna at the input of the receiver is 2.5 db including a polarization device.

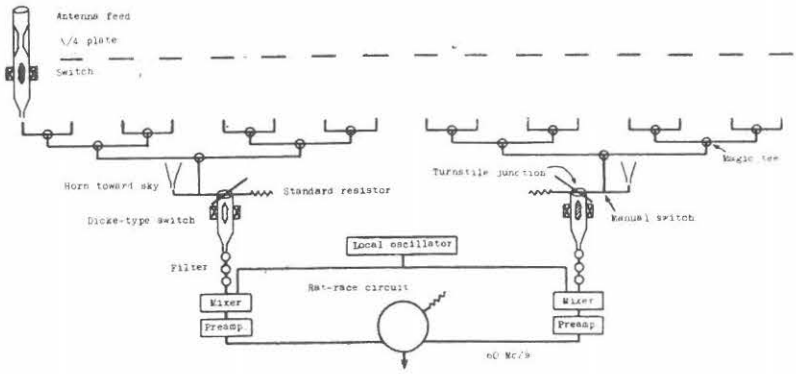

Fig. 2. Schematic diagram of combining antenna signals.

4. Receiver

Two Dicke-type ferrite switches are used at the input of the receiver with common

square-wave current, 500 c/s, flowing through the outer coil. By applying synchronous rectifier at the output of the receiver, we can get the record of R+L in parallel with R−L. Two mixers are fed by a common local oscillator which is frequency-controlled by a resonant cavity. Mixers and preamplifiers are carefully adjusted to secure similar performance. The band-width of the preamplifier is 10.5 Mc/s. A rat-race hybrid circuit is used to combine two outputs of the 8-element interferometers at the i-f stage. The band-width of the main i-f amplifier is reduced to 8.5 Mc/s to relieve the possible unbalance of the preamplifier stage. The overall band-width of the interferometer is therefore 8.5 Mc/s. Noise figure of the receiver measured just before the turnstile circuit in Fig. 2 is 11.5, which corresponds to the r-m-s output fluctuation[5] of 3° K for the time constant of 0.5 sec. This time constant is a compromise between fluctuation and the distortion of the drift curve that has a fundamental frequency of about 0.1 c/s. The actual apparent fluctuation is about 12 degrees peak-to-peak, that is 2.5 percent of the quiet sun level which oscillates between 130 and 610 dgrees.

5. Phase adjustment of the interferometer

Phase adjustment has been performed in the same way as is used for the interferometer at 4 Gc/s, i. e., the method of using the sun as a signal. Choosing a day when the sun is as quiet as possible, we take a series of drift curves by connecting the antenna two by two successively. Then, deviation from the theoretical values is calculated for each pair using a frequency measured from a drift curve of large beam numbers, say number 50 or more. The length of transmission lines are adjusted by inserting short waveguides between couplings. The error of 0.02 λ can be easily detected and corrected.

6. Tolerance of gain unbalance between two preamplifiers

The directive voltage pattern of the 16-element interferometer D_{16} can be written as,

$$D_{16}=\frac{1}{16}\ \frac{1-\varepsilon^{j16\varphi}}{1-\varepsilon^{j\varphi}}=\frac{1}{8}\ \frac{1-\varepsilon^{j8\varphi}}{1-\varepsilon^{j\varphi}}\cdot\frac{1+\varepsilon^{j8\varphi}}{2}=D_8\cdot\frac{1+\varepsilon^{j8\varphi}}{2} \quad \cdots\cdots(1)$$

where φ is the phase angle between inputs of the neighbouring antenna elements. It is quite clear that D_{16} is the product of two directive patterns, i. e., the directive pattern of 8-element interferometer D_8 and that of two-element interferometer with each element at the center of two 8 elements. From this fact, it is very easy to calculate the effect of gain unbalance between two preamplifiers. If the ratio of this voltage gain be γ which is less than a unity, equation (1) becomes,

$$D'_{16}=D_8\ \frac{1+\gamma\varepsilon^{j8\varphi}}{1+\gamma} \quad \cdots\cdots(2)$$

By numerical calculations, we can find that the first minimum of the power pattern rises by 0.12, 0.52 and 3.10 percent of the peak for the values of $\gamma=0.9$, 0.8 and 0.7 respectively. Thus gain unbalance of 20 percent may be tolerable, but we are trying to keep this unbalance within 10 percent, i. e. within 20 percent on the recorder chart.

III. Some results of observation

1. Structure of the source of polarization of S-component

We have found by eclipse observations[6] that the source of polarization is confined

over the sunspots and consequently the bipolar sunspot has two small sources of polarization over each sunspot. The change of the sense of polarization as a whole at a certain point on the course of travel over the solar surface may be due to the change of balance of these two sources[3]. This bipolar nature of the source of polarization was confirmed by using 2-element interferometer of large spacing at Nançay[7]. Observations by 16-element interferometer further support this structure, which is fairly clear when two sunspots

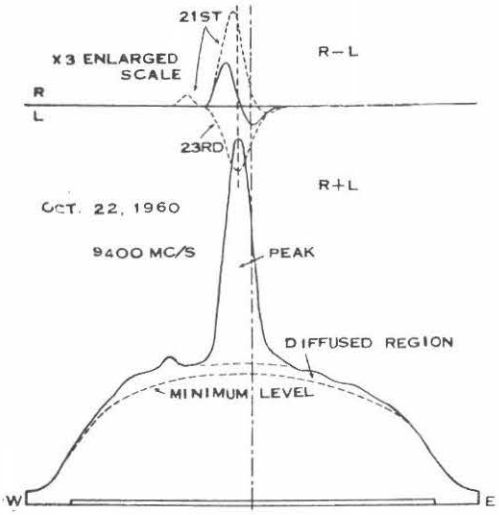

Fig. 3.—(a)
Typical drift curves for 9.4 Gc/s showing the existence of two sources of polarization in a small radio spot.

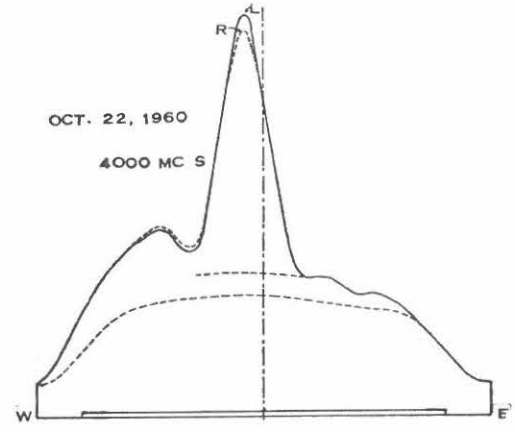

Fig. 3—(b)
Drift curves for 4 Gc/s on the same day.

separate by a few minutes of arc. Fig. 3-(a) is an example of the drift curve, both for R+L and R−L, showing the existence of two sources in a radio source as small as 2 minutes of arc. Two broken lines superposed on the drift curve of R−L are the similar drift curves on the neibouring days, shifted by putting the peaks of R+L on the same position. Minimum level in Fig. 3 is a lower envelope of superimposed drift curves through the months of October and November, 1960. The unsymmetry of this curve around the center line may be due to the tilt of the polar axis, which may be explained as caused by the shift of the equatorial bright region near the limb towards the north pole.

2. Size of the radio spot

The size of S (slowly varying) component was formerly measured by eclipse observations in 1955[8] and 1958[6] and we found that the bright region corresponds to the area of calcium plage at a frequency around 3000 Mc/s. On the other hand. M. R. Kundu[9] suggested the existence of some small bright regions corresponding to the sunspot area other than the broad patches over the solar surface at a frequency of 9.3 Gc/s. W. N. Christiansen and D. S. Mathewson showed a much broader feature of the radio source at 1400 Mc/s[10].

Since the regular observations by 16-element interferometer were started, there had been two large isolated spots on the sun, which were fabourable to knowing the size of the radio sources. The results are shown in Fig. 4. "The peak" is taken over the

diffused region, not over the minimum level, as shown in Fig. 3. The effective size of the source is estimated by assuming a rectangular uniform disk. Similar observations by 8-element interferometer at 4 Gc/s are also shown for comparison, though the resolving power in this case is half as poor. In Fig. 4, we can see that the size of the radio spots at 9.4 Gc/s is about 2 minutes of arc which corresponds closely to the area of the sunspots while the size at 4 Gc/s seems to be much broader. For 4 Gc/s, we have noticed for a long time that the shape of the peak on drift curves has a tendency of being triangular, as may be seen in Fig. 3-b. It may suggest that there will be a very bright region at this frequency over the sunpot surrounded by a less bright region corresponding to the calcium plage, placed over a more diffused background. The concentration may be much pronounced at higher frequencies and may become much oblique at lower frequencies around 1000 Mc/c[8] [6] [10]. These results may support the previous papers[8] [6] [9] [10] [13], when the variation of shape for different frequencies are taken into account. Heliographic observations by V. V. Vitkevich and others[11] are not available for this discussion because of the poorer resolving power of the antenna. V. Ikhsanova[12] has concluded that the size of the emitting region does not differ much from one minute of arc, but the figures he has shown seem to differ from his conclusion.

Another result that can be reduced from Fig. 4 is the center-limb variation of the size of a radio source. This reduction is very difficult because the error increases as the spot rotates towards the limb where the intensity diminishes and the minimum level is steep. It may be seen, however, that the size does not change remarkably during its travel across the sun, though a slight tendency is perceived of diminishing its size towards the limb at 9.4 Gc/s. This result is not the same as that of the Australian group[10], a disk-like model of S-region, probably due to the difference in frequency.

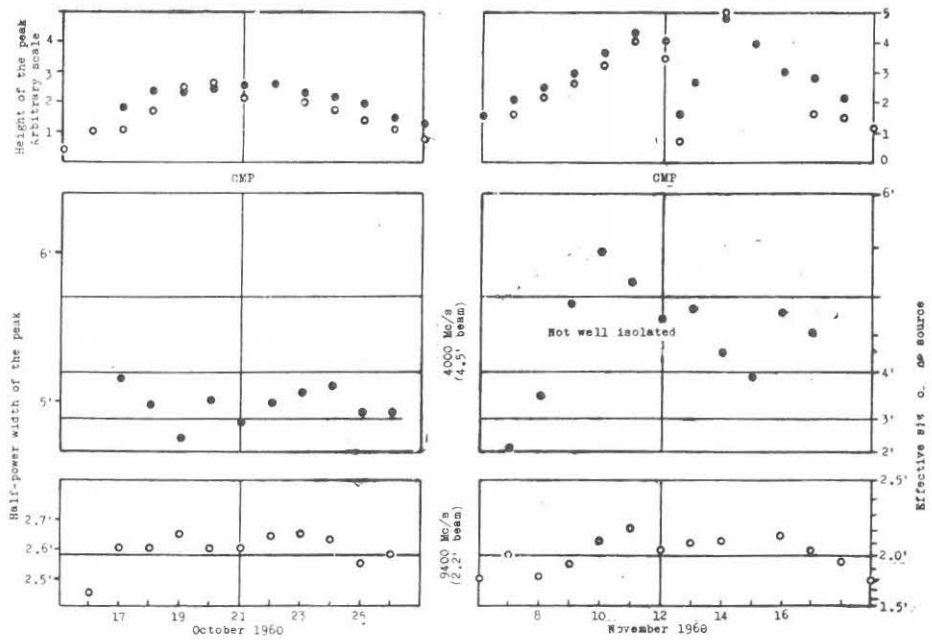

Fig. 4. Center-limb variation of intensity and size for two radio spots.

3. Movement of the source of polarization during the burst

On Nomber 11th, 14th and 15th, 1960, very intense bursts were observed at Toyokawa. In these bursts, it was found that the center of the source of polarization shifted appreciably during the 2nd phase of cm wave burst. In these cases, the center of brightness did not move within the accuracy of observations. This phenomenon suggests that there are two types of emissions on centimeter wavelength region. Datails are written in a separate paper in this volume (page 1).

IV. Acknowledgement

The author wishes to express his thanks to Messrs. T. Torii and Y. Tsukiji for their cooperation in constructing the interferometer, especially to Mr. T. Kakinuma for his command during the author's stay in France. Thanks are also due to Mr. T. Takayanagi and to all the staff of the Radio Astronomy Section here for their daily efforts for precise reductions of data. Finally, the author wishes to express his sincere thanks to the Director, Professor A. Kimpara, for his unceasing encouragement. (15th December, 1960).

References

(1) H. Tanaka: Proc. Res. Inst. Atmosph. Nagoya Univ., **6** (1959).
(2) H. Tanaka and T. Kakinuma: Proc. Res. Inst. Atmosph. Nagoya Univ., **2** & **3** (1954 & 5).
(3) H. Tanaka and T. Kakinuma: Proc. Res. Inst. Atmosph. Nagoya Univ., **7** (1960).
(4) H. Tanaka and T. Kakinuma: Proc. Res. Inst. Atmosph. Nagoya Univ., **5** (1958).
(5) H. Tanaka et al.: Proc. Res. Inst. Atmosph. Nagoya Univ., **1** (1953); Correction **2** (1954).
(6) H. Tanaka and T. Kakinuma: Rep. Ionosph. Res. Japan, **12**, 3 (1958).
(7) H. Tanaka and J.L. Steinberg: in preparation.
(8) T. Hatanaka, K. Akabane, F. Moriyama, H. Tanaka and T. Kakinuma: Rep. Ionosph. Res. Japan, **9** (1955); Publ. Astro. Soc. Japan, **7** (1955).
(9) M. R. Kundu: Annales d'Astrophysique, **22** (1959).
(10) W. N. Christiansen and D. S. Mathewson: Paris Symposium on Radio Astronomy, Stanford Unv. Press (1959).
(11) V. V. Vitkevich, A. D. Kuz'min, A. E. Salomonovich and V. A. Udal'tsov: ibid.
(12) V. Ikhsanova: ibid.
(13) A. E. Covington: Jour. Roy. Astro. Soc. Canada, **54** (1960).